International Journal of Nanomedicine

Dovepress
open access to scientific and medical research

Open Access Full Text Article

ORIGINAL RESEARCH

Alendronate-coated long-circulating liposomes containing ^{99m}technetium-ceftizoxime used to identify osteomyelitis

This article was published in the following Dove Press journal:
International Journal of Nanomedicine
25 March 2015
Number of times this article has been viewed

Diego dos Santos Ferreira[1]
Fernanda Alves Boratto[1]
Valbert Nascimento Cardoso[2]
Rogéria Serakides[3]
Simone Odília Fernandes[2]
Lucas Antônio Miranda Ferreira[1]
Mônica Cristina Oliveira[1]

[1]Department of Pharmaceutical Products, Faculty of Pharmacy, [2]Department of Clinical and Toxicological Analyses, Faculty of Pharmacy, [3]Veterinary School, Universidade Federal de Minas Gerais, Belo Horizonte, Minas Gerais, Brazil

Abstract: Osteomyelitis is a progressive destruction of bones caused by microorganisms. Inadequate or absent treatment increases the risk of bone growth inhibition, fractures, and sepsis. Among the diagnostic techniques, functional images are the most sensitive in detecting osteomyelitis in its early stages. However, these techniques do not have adequate specificity. By contrast, radiolabeled antibiotics could improve selectivity, since they are specifically recognized by the bacteria. The incorporation of these radiopharmaceuticals in drug-delivery systems with high affinity for bones could improve the overall uptake. In this work, long-circulating and alendronate-coated liposomes containing ^{99m}technetium-radiolabeled ceftizoxime were prepared and their ability to identify infectious foci (osteomyelitis) in animal models was evaluated. The effect of the presence of PEGylated lipids and surface-attached alendronate was evaluated. The bone-targeted long-circulating liposomal ^{99m}technetium–ceftizoxime showed higher uptake in regions of septic inflammation than did the non-long-circulating and/or alendronate-non-coated liposomes, showing that both the presence of PEGylated lipids and alendronate coating are important to optimize the bone targeting. Scintigraphic images of septic or aseptic inflammation-bearing Wistar rats, as well as healthy rats, were acquired at different time intervals after the intravenous administration of these liposomes. The target-to-non-target ratio proved to be significantly higher in the osteomyelitis-bearing animals for all investigated time intervals. Biodistribution studies were also performed after the intravenous administration of the formulation in osteomyelitis-bearing animals. A significant amount of liposomes were taken up by the organs of the mononuclear phagocyte system (liver and spleen). Intense renal excretion was also observed during the entire experiment period. Moreover, the liposome uptake by the infectious focus was significantly high. These results show that long-circulating and alendronate-coated liposomes containing ^{99m}technetium-radiolabeled ceftizoxime have a tropism for infectious foci.

Keywords: bone targeting, radiolabeled antibiotics, scintigraphic imaging, bone infection diagnosis

Introduction

Osteomyelitis is a bone infection that affects the bone marrow and adjacent cortical tissue, most commonly caused by pyogenic bacteria and mycobacteria, especially *Staphylococcus aureus*. It is a major complication that occurs after bone fractures and surgical treatments, and significantly affects patients' quality of life.[1–3] The diagnosis of this disease is most commonly performed on the basis of imaging, laboratory tests, and clinical examination.[4,5]

Nuclear medicine imaging allows for the in vivo detection of inflammatory and infectious diseases by the intravenous injection of radiolabeled substances followed by the external detection of radioactivity using a gamma camera. The sensitivity of this

Correspondence: Mônica Cristina Oliveira
Department of Pharmaceutical Products, Faculty of Pharmacy, Universidade Federal de Minas Gerais, Avenida Presidente Antônio Carlos, 6627 - Pampulha, Belo Horizonte, Minas Gerais, 31270-901, Brazil
Tel +55 31 3409 6945
Fax +55 31 3409 6935
Email monicacristina@ufmg.br; itabra2001@yahoo.com.br

submit your manuscript | www.dovepress.com
Dovepress
http://dx.doi.org/10.2147/IJN.S76168

technique usually allows for the detection of physiopathological processes in the initial stages before the development of anatomical alterations that are detectable by conventional radiographic techniques and the clinical onset of the disease, thus enabling a prompt installation of a proper therapy.[6]

The radiopharmaceuticals most commonly used for the imaging of bone inflammation and infection are ^{67}Gallium-citrate, ^{99m}Tc-methylene diphosphonate, and ^{99m}Tc-hexamethylpropyleneamine oxime-labeled autologous leukocytes. Although they are sensitive, their specificity for infection is low, as they accumulate in any area of inflammation.[7] Hence, there is a constant search for a new radiopharmaceutical that would allow for a rapid and efficient identification of infectious foci with a high level of sensitivity and specificity.[1,8] In this context, radiolabeled antibiotics that can be incorporated and metabolized by the bacteria present in the infectious foci, allowing for an accurate and specific identification of infectious sites, are of great interest.[8–11] Ceftizoxime (CFT) (Figure 1A) is a broad-spectrum antibiotic that binds to the bacterial cell wall and inhibits the formation of peptidoglycan, impairing the formation of the cell wall, and in turn killing the bacteria. Scintigraphic imaging studies have shown that CFT is able to identify a focus of bone infection and distinguish between septic and aseptic inflammation.[12] Another investigated approach for the diagnosis of infections is based on the use of radiolabeled liposomes. These drug-delivery systems have proven to be interesting carriers of imaging agents to identify infectious sites, since these areas have high blood flow and permeability that allow for the liposomes to extravasate and accumulate.[13–15] Despite that, radiolabeled liposomes are not able to differentiate septic from aseptic inflammation. In an effort to overcome the lack of specificity of radiolabeled liposomes and to improve the image quality, our research group has previously developed pH-sensitive liposomes containing ^{99m}technetium-radiolabeled CFT (^{99m}Tc-CFT) for the diagnosis of bone infections. This formulation demonstrated higher affinity for infectious sites than inflamed tissues, although the uptake was not increased, compared to the free ^{99m}Tc-CFT.[16] The explanation could be related to the fact that bones are poorly vascularized and composed mainly of mineral matrixes, which prevent most substances from reaching the region.[17] In light of this, the development of a surface-modified liposome by the incorporation of a ligand with high affinity for regions of intense bone turnover may be a promising strategy to increase the uptake of ^{99m}Tc-CFT at these regions and, consequently, improve the image quality. The application of active-targeted liposomes is well documented in the scientific literature. The modification of the liposomal surface can be performed by the insertion of antibodies, proteins, peptides, nucleic acids, sugars, and small molecules.[18] These ligands need to have a high affinity for substances that are overexpressed in the interest area, but are absent or poorly expressed in healthy tissues.[19] Among these ligands, transferrin, an internalizable iron-binding blood plasma glycoprotein, and folate, a vitamin, are the most successfully studied targeting moieties to increase the uptake of nanoparticles into transferrin and/or folate receptor overexpressing-tumors, such as ovarian, colon, breast, prostate, and renal tumors. Other examples of extensively applied ligands are cell-penetrating peptides (such as TAT [transactivator of transcription] or polyArg [polyarginine]), mannose, glucose, and the antibodies anti-CD19 and anti-HER2.[18,20] Specifically for bone targeting, bisphosphonates are among the drugs most capable of reaching the skeleton due to their calcium-chelating properties through their phosphonate groups.[21,22] Some authors have demonstrated the applicability of bisphosphonates as targeting moieties for drug-delivery systems. Anada et al developed an amphipathic molecule bearing a bisphosphonate headgroup (4-*N*-(3,5-ditetradecyloxy-benzoyl)-aminobutane-1-hydroxy-1,1-bisphosphonic acid disodium), and this compound was used to prepare conventional liposomes composed of distearoylphosphatidylcholine and cholesterol (Chol).[23]

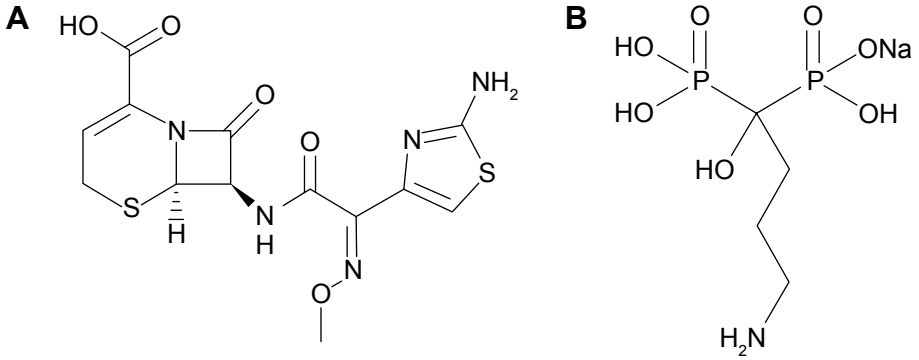

Figure 1 Chemical structure of ceftizoxime (**A**) and sodium alendronate (**B**).

Hengst et al synthetized a cholesteryl derivative attached to oxyethylene groups bearing a bisphosphonate headgroup and inserted this derivative into liposomes composed of egg phosphatidylcholine (EPC), Chol, and 1,2-distearoyl-*sn*-glycero-3-phosphoethanolamine-N-[(polyethylene glycol)-2000].[24] The insertion of bisphosphonates derivatives into the surface of poly(D,L-lactide-co-glycolide) nanoparticles has also been reached through the synthesis of a poly(d,l-lactide-co-glycolide) copolymer associated to polyethylene glycol and alendronate.[25] All these formulations demonstrated high in vitro affinity for hydroxyapatite. Swami et al demonstrated the capacity of the alendronate-coated poly(lactic-co-glycolic acid) nanoparticles to increase the uptake of the antitumor drug bortezomib into the bone marrow and inhibit the in vivo growth of multiple myeloma cells.[26] Despite the advantages of these bisphosphonates derivatives, their synthesis involves a multistep reaction. Thus, the conjugation of bisphosphonates to the drug-delivery systems' surface through a one-step reaction could be interesting, such as by means of ion pair formation.

Some studies have demonstrated the attachment of some hydrosoluble substances onto lipophilic nanoparticles by ion pair formation.[27,28] Stahl et al have presented two criteria that determine ion pairing to create insoluble salt forms. First, the difference in pKa between the acid and the base must be at least 2 pH units to ensure sufficient proton transfer. Second, the hydrophobic counter ions aid in the creation of insoluble ion pairs.[29] Association of water-insoluble 1,2-distearoyl-*sn*-glycero-3-phosphoethanolamine-N-[amino(polyethyleneglycol)-2000] (aPEG-DSPE) (pKa ~10.5) to water soluble alendronate (pKa ~3) (Figure 1B) may be an interesting strategy to attach this substance to the hydrophobic liposomal surface and create a bone-targeted (BT) formulation. Therefore, in the present study, we developed an alendronate-coated long-circulating liposomal formulation containing ^{99m}technetium labeled CFT (BT-CFT-LC-Lip). The lipid composition to achieve suitable ^{99m}Tc-CFT encapsulation was determined. The effect of the presence of PEGylated lipid and alendronate on image quality, and the applicability of this formulation in differentiating aseptic and septic inflammation, were evaluated.

Materials and methods

Materials

The CFT kits were kindly donated by the Laboratory of Radioisotopes (Universidade Federal de Minas Gerais, Belo Horizonte, Minas Gerais, Brazil). EPC and aPEG-DSPE were purchased from Lipoid GmbH (Ludwisgshafen, Germany). ^{99}Mo/^{99m}Tc generator was supplied by the Instituto de Pesquisas Energéticas e Nucleares (IPEN, São Paulo, São Paulo, Brazil). Sodium chloride (NaCl), Chol, stearylamine (SA), sodium alendronate, and zymosan were purchased from Sigma-Aldrich Co. (St Louis, MO, USA). Xylazine and ketamine solutions were acquired from Hertape Calier Saude Animal S/A (Juatuba, Minas Gerais, Brazil). The *S. aureus* cultures were supplied by the American Type Culture Collection (ATCC, Manassas, VA, USA).

CFT radiolabeling

The procedure used to label CFT was described previously.[30] Briefly, a kit containing 2.5 mg of CFT and 6.0 mg of sodium dithionite was reconstituted with 1.0 mL of sodium ^{99m}Tc-pertechnetate solution (Na $^{99m}TcO_4$) obtained by elution from a sterile ^{99}Mo/^{99m}Tc generator using sterile 0.9% w/v NaCl solution (370 MBq). The solution was boiled for 10 minutes and cooled under running water for 5 minutes. The solution was filtered through a cellulose ester filter (0.22 μm) to remove radiochemical contaminants, mainly reduced hydrolyzed technetium ($^{99m}TcO_2$), and collected in a vial under vacuum.

Radiochemical purity

The radiochemical purity (RP) of ^{99m}Tc-CFT was evaluated according to that described previously.[30] The ^{99m}Tc-CFT (3 μL) was applied to silica gel thin-layer chromatography plates and eluted with methyl ethyl ketone and 0.9% w/v NaCl solution to determine the amount of Na $^{99m}TcO_4$ and $^{99m}TcO_2$, respectively, by ascending chromatography. The radiation was measured in the beginning and at the end of the chromatography plate by an automatic scintillation apparatus model Wizard 3" 1480 covering an energy window of 140 keV (PerkinElmer Inc., Waltham, MA, USA). The RP was determined according to the following equation:

$$RP\,(\%) = \frac{\text{cpm of } {}^{99m}\text{TC-CFT}}{\text{cpm of } \left({}^{99m}TcO_2 + \text{Na } {}^{99m}TcO_4 + {}^{99m}\text{TC-CFT}\right)} \times 100 \quad (1)$$

Liposome preparation

For liposome preparation, the thin-film hydration method was initially applied. In brief, EPC, Chol, SA, and aPEG-DSPE at the total lipid concentration of 20 mM and variable molar ratios (Table 1) were solubilized in chloroform and submitted to evaporation under reduced pressure until a thin lipid film was obtained. The film was hydrated by adding the required amount of 0.9% w/v NaCl solution and dispersed by vortexing. The liposomes were submitted to the calibration by extrusion through polycarbonate membranes of porous sizes of 0.4, 0.2, and 0.1 μm (five passages for each).

Table 1 Lipid composition of the liposomes

Formulation	Molar ratio of lipids			
	EPC	Chol	SA	aPEG-DSPE
LipE	1	–	–	–
LipEC	0.8	0.2	–	–
LipES	0.8	–	0.2	–
LipECS I	0.4	0.3	0.3	–
LipECS II	0.64	0.16	0.2	–
LC-LipECS	0.6	0.15	0.19	0.05

Abbreviations: aPEG-DSPE, 1,2-distearoyl-*sn*-glycero-3-phosphoethanolamine-*N*-[amino(polyethylene glycol)-2000]; Chol, cholesterol; EPC, egg phosphatidylcholine; LC-LipECS, Long-circulating aPEG-DSPE:EPC:Chol:SA liposome; LipE, EPC liposome; LipEC, EPC:Chol liposome; LipECS I, EPC:Chol:SA liposome (low concentration of EPC); LipECS II, EPC:Chol:SA liposome (high concentration of EPC); LipES, EPC:SA liposome; SA, stearylamine.

After the preparation of the blank liposomes, ^{99m}Tc-CFT (2.5 mg/mL) was added to the extruded liposomes. The mixture was frozen in liquid N_2 for 5 minutes and thawed at 37°C for 5 minutes. The freeze–thaw step was repeated three times. The untrapped ^{99m}Tc-CFT was then separated by ultracentrifugation (150,000× *g*, 90 minutes, 4°C). The pellet was suspended in 0.9% w/v NaCl solution to form alendronate-non-coated liposomes containing ^{99m}Tc-CFT. LipECS II (EPC:Chol:SA liposome [high concentration of EPC]) and LC-LipECS (long-circulating aPEG-DSPE:EPC:Chol:SA liposome) were also incubated with 0.9% w/v NaCl solution and sodium alendronate (1.0 mg/mL) to form alendronate-coated liposomes containing ^{99m}Tc-CFT (BT LipECS II containing ^{99m}Tc-CFT [BT-CFT-Lip] and BT-CFT-LC-Lip, respectively). Both dispersions were maintained under mechanical stirring for 1 hour.

Liposome characterization

The liposomes were characterized by their encapsulation percentage (EP), size, polydispersity index (PDI), and zeta potential. The EP of CFT into liposomes was determined by the quantification of gamma radiation in non-purified and purified liposomes. The radioactivity was measured by an automatic scintillation apparatus model Wizard 3" 1480 covering an energy window of 140 keV (PerkinElmer Inc.). The counting time was 1 minute. The EP was calculated by means of the following equation:

$$EP(\%) = \frac{^{99m}\text{Tc-CFT amount in purified liposomes}}{^{99m}\text{Tc-CFT amount in non-purified liposomes}} \times 100 \quad (2)$$

The mean diameter and PDI of liposomes was determined by means of quasielastic light scattering at 25°C and an angle of 90°. The zeta potential was evaluated by determining the electrophoretic mobility at an angle of 90°. All samples were diluted in a 1 mM NaCl solution, and the measurements were performed in triplicate using the 3000HS Zetasizer equipment (Malvern Instruments, Malvern, UK). The incorporation of alendronate to the liposomal surface has been assumed considering variations in mean diameter, PDI, and zeta potential as well as the in vivo results.

Experimental animal model

During the procedure, the Wistar male rats (180–220 g) were anesthetized with a mixture of xylazine (8 mg/kg) and ketamine (60 mg/kg) by intraperitoneal route, and the legs were disinfected with a 1% w/v tincture of iodine. The experimental rat model of acute osteomyelitis was developed by direct inoculation of 0.2 mL containing 10^8 colony-forming units of *S. aureus* (ATCC 6538-P) into the medullar cavity of the left tibia without sclerosants. In addition, sterile inflammatory foci were induced by the direct inoculation of 0.2 mL of zymosan (*Saccharomyces cerevisiae*) in sterile saline into the medullar cavity of the left tibia. Likewise, 0.2 mL of sterile saline was injected into the medullar cavity of the left tibia in the control group. All protocols were approved by the Ethics Committee for Animal Experiments at Universidade Federal de Minas Gerais (protocol number 237/10) and are in compliance with the guide for the care and use of laboratory animals recommended by the Institute of Laboratory Animal Resources. The development of infectious and inflammatory foci were confirmed by histological studies, in accordance with that previously described.[12]

Evaluation of the effect of PEGylation and alendronate-coating on the identification of infectious foci by scintigraphic images

Forty-eight hours after the induction of the infectious foci, 200 µL (approximately 20 MBq) of Lip ECS II containing ^{99m}Tc-CFT (CFT-Lip), LC-LipECS containing ^{99m}Tc-CFT (CFT-LC-Lip), BT-CFT-Lip, or BT-CFT-LC-Lip were injected into the tail vein of the rats (five per group). At preestablished times (1, 2, 4, 6, and 8 hours), the animals were anesthetized with a mixture of xylazine (8 mg/kg) and ketamine (60 mg/kg) by intraperitoneal injection and placed in the prone position on a gamma camera equipped with a low-energy collimator Nuclide TH 22 (Mediso, Budapest, Hungary). Ten-minute static planar images were acquired using a 256×256 pixel matrix. The scintigraphic images were analyzed in the regions of interest by outlining the infected or inflamed left tibia (target). These regions of interest were automatically copied to the contralateral tibia (non-target). The target-to-non-target ratios were calculated using the total counts.

Evaluation of the differentiation ability of septic and aseptic inflammatory foci by BT-CFT-LC-Lip

Forty-eight hours after the induction of acute osteomyelitis and sterile inflammation, approximately 20 MBq of BT-CFT-LC-Lip was injected into the tail vein of the rats (five per group). At preestablished times (1, 2, 4, 6, and 8 hours), the animals were anesthetized with a mixture of xylazine (8 mg/kg) and ketamine (60 mg/kg) by intraperitoneal injection and placed in the prone position on a gamma camera equipped with a low-energy collimator Nuclide TH 22 (Mediso). Ten-minute static planar images were acquired using a 256×256 pixel matrix. The quantitative analyses were carried out as described above.

Ex vivo biodistribution study

Samples containing approximately 20 MBq of BT-CFT-LC-Lip (200 µL) were injected intravenously into the tail vein of osteomyelitis-bearing Wistar rats. After periods of 1, 2, 4, 6, and 8 hours, each animal (five per group) was anesthetized intraperitoneally with a mixture of ketamine and xylazine at a dose of 60 and 8 mg/kg, respectively. The blood was collected immediately by cardiac puncture, and the rats were sacrificed by cervical dislocation. The lungs, spleen, liver, kidneys, and right and left tibias were collected, washed with distilled water, dried on filter paper, and weighed. The determination of radioactivity amount in the organs was achieved through quantification on an automatic scintillation apparatus model Wizard 3″ 1480 covering an energy window of 140 keV (PerkinElmer Inc.). The readings were conducted for 1 minute. The results were expressed as the percentage of injected dose/g of tissue. A standard dosage containing the same injected amount was counted simultaneously in a separate tube, which was taken as 100% of radioactivity.

Statistical analysis

The results were calculated and presented as the mean ± standard error of mean. The difference among experimental groups was tested using the one-way analysis of variance test, followed by Newman–Keuls' multiple test or Tukey's test to obtain a variable with a variation coefficient of higher or lower than 15%, respectively. The software GraphPad Prism version 5.0 (GraphPad Software, Inc., La Jolla, CA, USA) was used. Differences were considered statistically significant when *P*-values were lower than 0.05.

Results and discussion

RP

The labeling yield of the ^{99m}Tc-CFT was 79.5%±1.3%. The contents of $^{99m}TcO_2$ and $Na^{99m}TcO_4$ were 17.1%±1.8% and 3.4%±0.9%, respectively. The $^{99m}TcO_2$ is a colloid that is insoluble in water and that is phagocytosed by mononuclear phagocytic system organs, mainly the liver and the spleen. The presence of this impurity does not compromise the quality of the images since they are focused on the tibia. The $Na^{99m}TcO_4$ is distributed through vessels and intestinal fluids. It accumulates in the gastrointestinal tract, thyroid, and salivary glands, resulting in increased activity in these organs.[31] Radiochemical impurities may result in poor-quality images due to a high background radiation around the tissues and blood.[32] However, this result will not occur in the case of use of ^{99m}Tc-CFT when used to identify the presence of infection in the tibia region. Furthermore, the results demonstrated good RP.

Liposome characterization

Non-BT liposomes

The mean diameter, PDI, zeta potential, and EP are represented in Table 2. All formulations presented mean diameters of below 200 nm. Studies have demonstrated that small liposomes (100–200 nm) remain in blood circulation for a longer span of time, resulting in an increased accumulation at sites of focal infection. Moreover, these liposomes have the ability to leak from blood vessels, reaching the region of interest.[33–36] In contrast, large liposomes are not retained in infectious sites, as they are rapidly cleared from circulation by the organs of the mononuclear phagocyte system.[15] Therefore, the small size of the liposomes used in the study was adequate for the scintigraphic detection of the infection sites. The higher mean diameter for the formulation LipECS I (EPC:Chol:SA liposome [low concentration of EPC]) could be related to the small quantity of liposome-forming lipid EPC. It is well known that, ideally, the amount of this lipid shall vary between 60% and 70% of total lipids and the reduction could lead to nonlamellar structure formation.[37] The PDI of the formulations varied from 0.1 to 0.3, which means that the formulations are homogeneous. The zeta potential varied from –2 to 34 mV. This variation is related to the presence or absence of charged lipids. Liposomes composed of noncharged lipids, such as EPC and Chol, are slightly negative due to the presence of residual acidic lipid contaminants.[38] The insertion of positively charged lipids, such as SA and aPEG-DSPE, lead to the increasing of the zeta potential. This increase is proportional to the amount of positively-charged

Table 2 Physicochemical characteristics of the formulations after incorporation of ^{99m}Tc-CFT

Formulation	Mean diameter (nm)	PDI	Zeta potential (mV)	Entrapment percentage (%)
Non-bone-targeted formulations				
LipE	146±8[a]	0.34±0.02[a]	−2.3±1.0[a]	2.6±3.1[a]
LipEC	139±10[a,c]	0.33±0.05[a]	−3.1±2.1[a]	6.2±2.4[a,b]
LipES	137±6[a,c]	0.29±0.06[a,d]	14.8±3.4[b]	6.8±3.4[a,b]
LipECS I	176±7[b]	0.14±0.04[b]	24.7±2.9[c]	10.3±3.2[b]
LipECS II	126±6[c]	0.13±0.02[b,c]	17.9±4.1[b,c]	22.8±1.4[c]
LC-LipECS	139±12[a,c]	0.18±0.01[b,d]	33.9±2.9[d]	39.5±5.3[d]
Bone-targeted formulations				
BT-CFT-Lip	152±7*	0.17±0.03	10.9±2.2*	–
BT-CFT-LC-Lip	187±23*	0.23±0.03	21.5±0.5*	–

Notes: These results are expressed as mean ± standard deviation (n=3). Different superscript letters represent statistically significant difference ($P<0.05$). *Significant difference between BT-CFT-Lip, BT-CFT-LC-Lip, and their alendronate non-coated formulations (LipECS II and LC-LipECS, respectively). *P*-values less than 0.05 were set as the level of significance.

Abbreviations: BT-CFT-LC-Lip, alendronate-coated long-circulating liposomal formulation containing ^{99m}technetium labeled CFT; CFT, ceftizoxime; PDI, polydispersity index; BT-CFT-Lip, alendronate-coated liposomal formulation containing ^{99m}technetium labeled CFT; LipE, EPC liposome; LipEC, EPC:Chol liposome; LipES, EPC:SA liposome; LipECS I, EPC:Chol:SA liposome (low concentration of EPC); LipECS II, EPC:Chol:SA liposome (high concentration of EPC); LC-LipECS = Long circulating aPEG-DSPE:EPC:Chol:SA liposome.

lipid added. Zeta potential is an important parameter to predict the long-term stability of colloidal formulations. Generally, zeta potential values of 25 mV (absolute value) and above characterize a stable formulation, since the aggregation of the particles is less likely to occur due to electrical repulsion forces.[37] Two of the formulations presented zeta potential values at this range (LipECS I and LC-LipECS). The entrapment percentage varied from 3% to 40%. This variation can be related to the variable organization of lipid bilayers in fluid or rigid structures. It is well known that rigid structures are able to better retain the entrapped drug.[37]

The formulations LipE (EPC liposome), LipEC (EPC:Chol liposome), and LipES (EPC:SA liposome) presented suitable diameter and PDI, but the values of zeta potential and EP were low, which may compromise the long-term stability and reduce the ^{99m}Tc-CFT uptake into the region of interest, respectively. Despite the high value of zeta potential of LipECS I, this formulation presented a low value of EP. On the other hand, LipECS II showed a smaller value of zeta potential than LipECS I, which could compromise the long-term stability of the formulation. However, LipECS II presented suitable average diameter and EP to be applied for identification of bone infections. LC-LipECS demonstrated adequate average diameter and PDI, and high zeta potential. The high amount of ^{99m}Tc-CFT encapsulated in LC-LipECS can lead to a better uptake of the radiopharmaceutical into the infectious region. Considering all of the factors discussed above, LipECS II and LC-LipECS were chosen to be attached to the alendronate, forming BT-CFT-Lip and BT-CFT-LC-Lip, respectively.

Bone targeted liposomes

Both formulations showed an increase of the mean diameter after incorporation of alendronate. This increase can be indicative of alendronate anchoring to the liposome surface. Other reasons for this event, such as aggregation, can be excluded since the PDI values of the formulations did not change. In addition, the decrease of the zeta potential values, compared to the alendronate-non-coated formulations, is suggestive of the occurrence of electrostatic interactions between positively charged amine groups of SA molecules and negatively charged phosphate groups of alendronate molecules on the surface of liposomes.

Scintigraphic images

Evaluation of the effect of PEGylation and alendronate coating on the identification of infectious foci by scintigraphic images

First, the impact of the presence of PEGylated lipid and alendronate on the surface of liposomes was evaluated with regard to their uptake in the infectious foci. The values of the target-to-non-target ratios are shown in Figure 2.

Both long-circulating liposomal formulations presented a higher uptake in the infectious foci when compared to the non-long-circulating liposomes. The target-to-non-target ratio for BT-CFT-LC-Lip varied from 2.3 to 3.0 between 1 and 8 hours, while for BT-CFT-Lip this value was maintained at around 1.3 throughout the investigated time interval. The same pattern could be observed when analyzing the non-targeted liposomes. The target-to-non-target ratio for CFT-LC-Lip varied from 1.5 to 1.8 while for CFT-Lip this ratio was maintained at around 1 during the whole time interval. Several studies have been demonstrating the importance of the incorporation of PEGylated lipids onto the liposomal surface in order to increase the blood half-life and, consequently, uptake in the region of interest.[39,40] When considering the effect of alendronate-surface coating for both non- and long-circulating

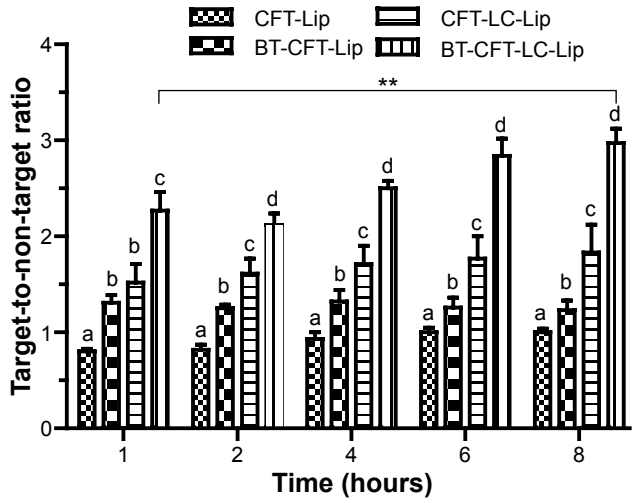

Figure 2 Quantitative analysis of scintigraphic images of osteomyelitis-bearing Wistar rats after intravenous injection of various formulations.
Notes: The letters a, b, c, and d indicate statistically significant difference between groups for each time interval ($P<0.05$). The **indicates statistically significant difference between 1 and 8 hours for the BT-CFT-LC-Lip ($P<0.01$).
Abbreviations: BT-CFT-LC-Lip, alendronate-coated long-circulating liposomal formulation containing ^{99m}technetium labeled CFT; CFT, ceftizoxime; CFT-LC-Lip, LC-LipECS containing ^{99m}Tc-CFT; CFT-Lip, LipECS II containing ^{99m}Tc-CFT; BT-CFT-Lip, alendronate-coated liposomal formulation containing ^{99m}technetium labeled CFT; LipE, EPC liposome; LipEC, EPC:Chol liposome; LipES, EPC:SA liposome; LipECS I, EPC:Chol:SA liposome (low concentration of EPC); LipECS II, EPC:Chol:SA liposome (high concentration of EPC); LC-LipECS = Long circulating aPEG-DSPE:EPC:Chol:SA liposome.

formulations, the presence of alendronate molecules increased the target-to-non-target ratio. This can be explained by a higher uptake of the liposomes in the bone, due to the specific interaction of the bisphosphonate molecules with hydroxyapatite molecules through their P-C-P moiety.[21]

Potential diagnostic agents should provide a target-to-non-target ratio of greater than 1.5 (50% higher uptake in the target tissue).[41] Both long-circulating liposomal formulations (BT-CFT-LC-Lip and CFT-LC-Lip) presented a target-to-non-target ratio of above this value throughout the investigated time interval. However, higher values were obtained after the administration of BT-CFT-LC-Lip. It is also important to notice a significant improvement of the target-to-non-target ratio for this formulation throughout the time interval, which can be useful to generate cleaner images at later acquisition time. Accordingly with these results, it is possible to suggest that both the longer circulation time, achieved by the incorporation of aPEG-DSPE, and the active bone targeting, achieved by the surface coating with alendronate molecules, are important to increase the uptake and residence time of the liposomes into the infectious foci, allowing the local release of ^{99m}Tc-CFT and improving of the image quality.

Previous studies have demonstrated high affinity of bisphosphonate-surface-coated nanoparticles for hydroxyapatite.[23,25] Nevertheless, to our knowledge, this is the first time that the high BT liposomal drug uptake is demonstrated by means of imaging (Figure 3). The animals injected with BT-CFT-LC-Lip presented a higher uptake of ^{99m}Tc-CFT when compared to the non-targeted liposomes. It is also possible to observe more clearly an increment on signal/noise ratio throughout the evaluated time interval. This effect can be explained by the high affinity of the BT liposomes for regions of high bone turnover. Since these liposomes are able to anchor to these regions by complexation with calcium ions, they accumulate and deliver ^{99m}Tc-CFT more efficiently than the non-targeted liposomes. This effect facilitates the precise localization of the

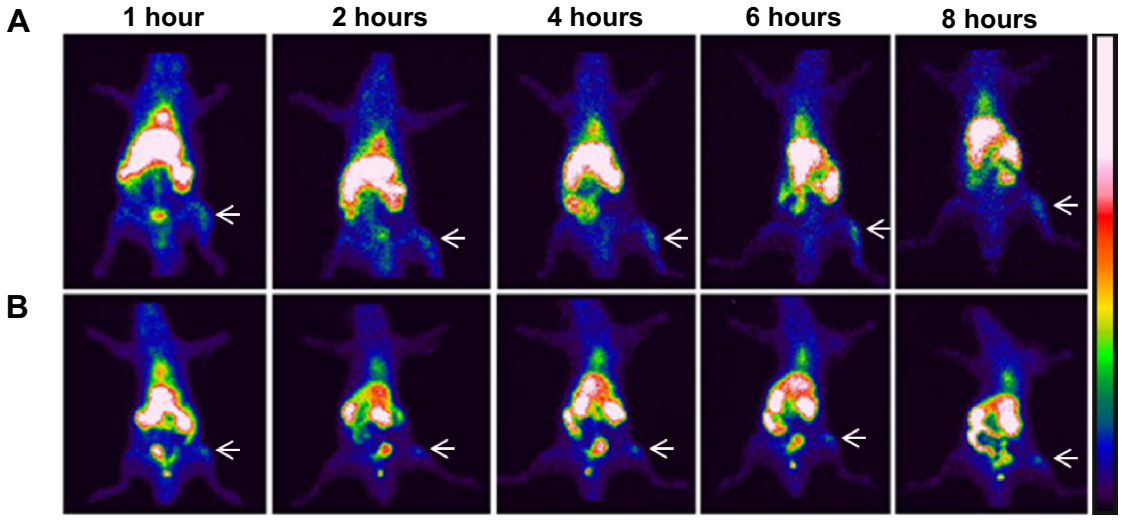

Figure 3 Scintigraphic images of rats infected with *S. aureus* (anterior view) after intravenous injection of BT-CFT-LC-Lip (**A**) or CFT-LC-Lip (**B**).
Notes: The images were taken at intervals of 1, 2, 4, 6, and 8 hours. The white arrows indicate the location of the infectious focus.
Abbreviations: BT-CFT-LC-Lip, alendronate-coated long-circulating liposomal formulation containing ^{99m}technetium labeled CFT; CFT, ceftizoxime; CFT-LC-Lip, LC-LipECS containing ^{99m}Tc-CFT; LC-LipECS, Long circulating aPEG-DSPE:EPC:Chol:SA liposomes.

infectious foci throughout the whole time interval. The difference of the target-to-non-target ratios between BT-CFT-LC-Lip- or CFT-LC-Lip-treated animals was more pronounced at the time interval of 6 hours (2.81±0.24 and 1.76±0.28, respectively) (Figure 2). The same pattern was observed when compared the non-long-circulating liposomes, BT-CFT-Lip and CFT-Lip (data not shown).

The scintigraphic images also showed a high uptake of liposomal formulations by the liver and spleen. This fact can be explained by the opsonization of the formulation and recognition by the mononuclear phagocytic system.[42] In none of the experimental groups investigated could the uptake of radioactivity by the thyroid gland be observed, illustrating that the liposomes have a high degree of RP and in vivo stability.

Evaluation of the differentiation ability of septic and aseptic inflammatory foci by BT-CFT-LC-Lip

We also evaluated the ability of BT-CFT-LC-Lip to differentiate septic from aseptic inflammation. A higher uptake of liposomal ^{99m}Tc-CFT was detected in the left tibia of osteomyelitis-bearing animals when compared to administration in aseptic inflammation-bearing and healthy animals (Figure 4).The target-to-non-target ratios varied from 2.3 to 3.0 between 1 and 8 hours for the osteomyelitis-bearing animals. The aseptic inflammation-bearing rats presented a variation from 1.4 to 2.0, while in the control group these values were maintained at around 1.0 during the whole time interval.

These results suggest that three factors may act in the uptake of the radiopharmaceutical in the region of interest. First, the region affected by inflammation (both septic and aseptic) present increased blood flow and vascular permeability, allowing for leakage and the maintenance of liposomes due to the permeation and retention effect, since these systems have a lower diameter than the pores of the vessels.[14] Moreover, the presence of alendronate on the surface promotes bone uptake, since this drug has a high affinity for hydroxyapatite.[35] These two factors explain the accumulation of the radiopharmaceutical in the regions of both septic and aseptic inflammation. However, the release of ^{99m}Tc-CFT and specific binding of the radiopharmaceutical to bacteria allows for a greater accumulation in the regions of interest in the septic inflammation model, in turn leading to a higher target-to-non-target ratio.

Biodistribution studies

The biodistribution profile of BT-CFT-LC-Lip administered intravenously in osteomyelitis-bearing Wistar rats was evaluated. An intense uptake of BT-CFT-LC-Lip by the spleen, as well as high and constant renal clearance, could be observed at all time intervals (Figure 5). An important uptake of BT-CFT-LC-Lip by the liver was also observed. These results are consistent with those observed by the scintigraphic images and previously described by our research group after injection of ^{99m}Tc-labeled long-circulating pH-sensitive liposomes in experimental infection models.[14]

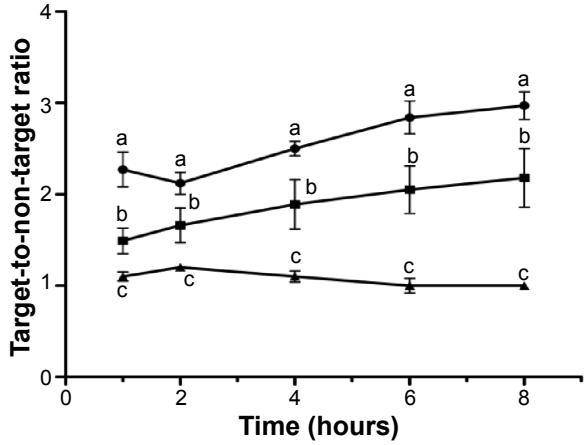

Figure 4 Quantitative analysis of scintigraphic images.
Notes: Quantitative analysis of scintigraphic images of healthy- (▲), osteomyelitis bearing- (●), and aseptic inflammation bearing- (■) Wistar rats after intravenous injection of BT-CFT-LC-Lip. The results are expressed as mean ± standard deviation (n=5). The letters a, b, and c indicate statistically significant difference between groups for each time interval ($P<0.05$).
Abbreviation: BT-CFT-LC-Lip, alendronate-coated long-circulating liposomal formulation containing ^{99m}technetium labeled ceftizoxime.

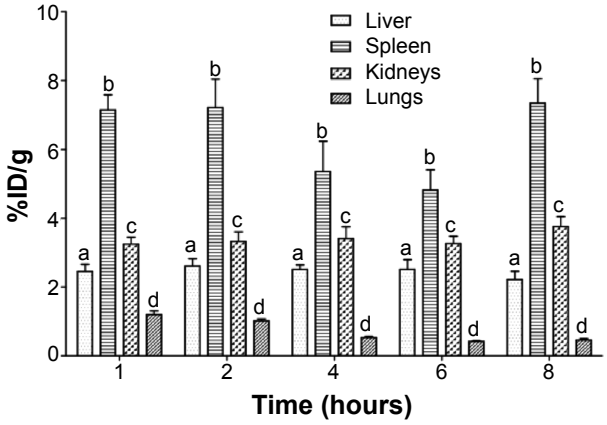

Figure 5 Concentration profile of ^{99m}Tc-CFT in liver, spleen, kidneys, and lungs after intravenous administration of BT-CFT-LC-Lip in osteomyelitis-bearing rats.
Note: The results are expressed as mean ± standard error (n=5). The letters a, b, c, and d indicate statistically significant difference between organs for each time interval ($P<0.05$).
Abbreviations: BT-CFT-LC-Lip, alendronate-coated long-circulating liposomal formulation containing ^{99m}technetium labeled CFT; CFT, ceftizoxime; %ID/g, percentage of injected dose per gram.

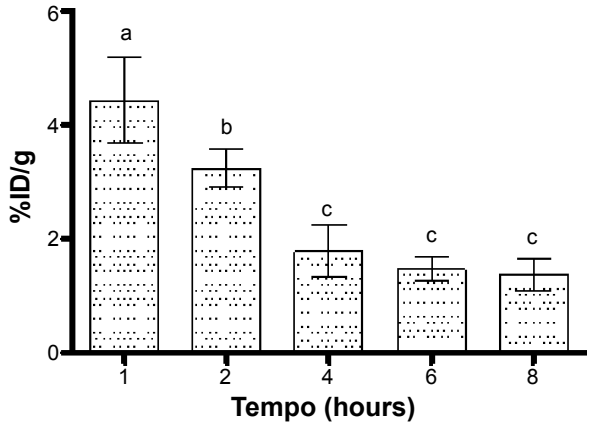

Figure 6 Concentration profile of ^{99m}Tc-CFT in blood after intravenous administration of BT-CFT-LC-Lip in osteomyelitis-bearing Wistar rats.
Notes: The results are expressed as mean ± standard error (n=5). Different letters indicate statistically significant differences between the times analyzed ($P<0.05$).
Abbreviations: BT-CFT-LC-Lip, alendronate-coated long-circulating liposomal formulation containing ^{99m}technetium labeled CFT; CFT, ceftizoxime; %ID/g, percentage of injected dose per gram.

The uptake of BT-CFT-LC-Lip by the liver and the spleen can be explained by its elimination by the mononuclear phagocyte system.[42] The high radioactivity detected in the kidneys at the first studied time interval can be attributed to the elimination of free ^{99m}Tc-CFT, since this antibiotic presents a half-life of approximately 1.5 hours and is excreted by the kidneys in active form (unchanged).[43] At later time intervals, given that the splenic and hepatic metabolism of liposomes occurs, as does the consequent release of ^{99m}Tc-CFT in the bloodstream, this radiopharmaceutical becomes available for excretion, maintaining constant renal elimination. The pulmonary uptake of BT-CFT-LC-Lip, when compared to the other organs, was low and proved to decrease over time.

In the bloodstream, the maximum BT-CFT-LC-Lip uptake occurred at 1 hour after injection (Figure 6). After 1 hour, BT-CFT-LC-Lip levels decreased over time, which can be explained by the significant hepatic and spleen uptake of liposomes followed by the renal elimination during the evaluated time interval.

The uptake of liposomes in the left tibia remained constant during all analyzed time intervals, while the uptake in the right tibia (healthy) decreased (Table 3). The maintenance of the radioactivity in the left tibia is consistent with the specific recognition and uptake of antibiotics by bacteria, presenting consistently high levels in the area. On the other hand, the uptake of BT-CFT-LC-Lip in the right tibia showed a decrease, which is directly related to the elimination of ^{99m}Tc-CFT.

Table 3 Concentration (%ID/g) profile of ^{99m}Tc-CFT in tibia after intravenous administration of BT-CFT-LC-Lip in osteomyelitis-bearing Wistar rats

Organ	Time post-injection (hours)				
	1	2	4	6	8
Left tibia	0.56 ± 0.07^{a}	0.57 ± 0.05^{a}	0.44 ± 0.07^{a}	0.49 ± 0.03^{a}	0.51 ± 0.08^{a}
Right tibia	0.37 ± 0.03^{b}	0.33 ± 0.04^{b}	$0.22\pm0.04^{b,*}$	$0.22\pm0.02^{b,*}$	$0.21\pm0.04^{b,*}$

Notes: The results are expressed as mean ± standard error (n=5). Different letters indicate statistically significant differences between the tibias in the same time interval ($P<0.05$). *Statistically significant differences of ^{99m}Tc-CFT concentration at the determined time point compared to the initial time ($P<0.05$).
Abbreviations: BT-CFT-LC-Lip, alendronate-coated long-circulating liposomal formulation containing ^{99m}technetium labeled CFT; CFT, ceftizoxime; %ID/g, percentage of injected dose per gram.

Conclusion

In this study, we proved the importance of association of both long-circulation and active bone-targeting by the surface-anchoring of alendronate molecules to achieve a high liposomal ^{99m}Tc-CFT uptake in bone infectious sites. The formulation BT-CFT-LC-Lip could improve the target-to-non-target ratios in septic inflammation compared to the previously reported results for free CFT or long-circulating and pH-sensitive liposomal-formulation containing CFT, especially in later acquisition times. In addition, this formulation was able to differentiate septic from aseptic inflammation. Therefore, these results indicate that the attachment of alendronate to the liposomal membrane can be a suitable strategy to improve the drug uptake for diagnosis and treatment of bone diseases.

Acknowledgments

The authors would like to thank FAPEMIG, CNPq, and FINEP for their financial support. Diego dos Santos Ferreira wishes to thank CNPq for his grant.

Disclosure

The authors report no conflicts of interest in this work.

References

1. El-Manghraby TA, Moustafa HM, Pauwels EK. Nuclear medicine methods for evaluation of skeletal infection among other diagnostic modalities. *Q J Nucl Med Mol Imaging*. 2006;50:167–192.
2. Kothari NA, Pelchovitz DJ, Meyer JS. Imaging of musculoskeletal infections. *Radiol Clin North Am*. 2001;39:653–671.
3. Lang S. [Osteomyelitis: a pathomorphologic overview]. *Radiologe*. 1996;36:781–785. German.
4. Rennen HJ, Boerman OC, Oyen WJ, Corstens FH. Imaging infection/inflammation in the new milennium. *Eur J Nucl Med*. 2001;28:241–252.
5. Gratz S, Rennen HJ, Boerman OC, Oyen WJ, Burma P, Corstens FH. (99m)Tc-interleukin-8 for imaging of acute osteomyelitis. *J Nucl Med*. 2001;42:1257–1264.
6. Signore A, D' Alessandria C, Annovazzi A, Scopinaro F. Radiolabeled cytokines for imaging chronic inflammation. *Brazilian Archives of Biology and Technology*. 2002;45:15–23.

7. Palestro CJ, Love C, Miller TT. Diagnostic imaging tests and microbial infections. *Cell Microbiol*. 2007;9:2323–2333.
8. Love C, Palestro CJ. Radionuclide imaging of infection. *J Nucl Med Technol*. 2004;32:47–57.
9. Benitez A, Roca M, Martin-Comin J. Labeling of antibiotics for infection diagnosis. *Q J Nucl Med Mol Imaging*. 2006;50:147–152.
10. Pineda C, Vargas V, Rodríguez AV. Imaging of osteomyelitis: current concepts. *Infect Dis Clin North Am*. 2006;20:789–825.
11. Wareham D, Michael J, Das S. Advances in bacterial specific imaging. *Brazilian Archives of Biology and Technology*. 2005;48:145–152.
12. Diniz SO, Rezende CM, Serakides R, et al. Scintigraphic imaging using technetium-99m-labeled ceftizoxime in an experimental model of acute osteomyelitis in rats. *Nucl Med Commun*. 2008;29:830–836.
13. Boerman OC, Dans ET, Oyen WJ, Corstens FH, Storm G. Radiopharmaceuticals for scintigraphic imaging of infection and inflammation. *Inflamm Res*. 2001;50:55–64.
14. Carmo VAS, de Oliveira MC, Mota LG, Freire LP, Ferreira RLB, Cardoso VN. Technetium-99m-labeled stealth pH-sensitive liposomes: a new strategy to identify infection in experimental model. *Brazilian Archives of Biology and Technology*. 2007;50:199–207.
15. Oyen WJ, Boerman OC, Storm G, et al. Detecting infection and inflammation with technetium-99m-labeled Stealth liposomes. *J Nucl Med*. 1996;37:1392–1397.
16. Ferreira SM, Domingos GP, Ferreira Ddos S, et al. Technetium-99m-labeled ceftizoxime loaded long-circulating and pH-sensitive liposomes used to identify osteomyelitis. *Bioorg Med Chem Lett*. 2012;22:4605–4608.
17. Rogers MJ. From molds and macrophages to mevalonate: a decade of progress in understanding the molecular mode of action of bisphosphonates. *Calcif Tissue Int.* 2004;75:451–461.
18. Bertrand N, Wu J, Xu X, Kamaly N, Farokhzad OC. Cancer nanotechnology: the impact of passive and active targeting in the era of modern cancer biology. *Adv Drug Deliv Rev*. 2014;66:2–25.
19. Wang G, Thanou M. Targeting nanoparticles to cancer. *Pharmacological Research*. 2010;62:90–99.
20. Torchilin VP. Targeted pharmaceutical Nnanocarriers for cancer therapy and Imaging. *AAPS J*. 2007;9:E128–E147.
21. Russel RG, Watts NB, Ebetino FH, Rogers MJ. Mechanisms of action of biphosphonates: similarities and differences and their potential influence on clinical efficacy. *Osteoporosis Int*. 2008;19:733–759.
22. Schott H, Goltz D, Schott TC, Jauch C, Schwendener RC. N^4-[Alkyl-(hydroxyphosphono)phosphonate]-cytidine-new drugs covalently linking antimetabolites (5-FdU, araU or AZT) with bone-targeting bisphosphonates (alendronate or pamidronate). *Bioorg Med Chem*. 2011;19:3520–3526.
23. Anada T, Takeda Y, Honda Y, Sakurai K, Suzuki O. Synthesis of calcium phosphate-binding liposome for drug delivery. *Bioorg Med Chem Lett*. 2009;19:4148–4150.
24. Hengst V, Oussoren C, Kissel T, Storm G. Bone targeting potential of bisphosphonate-targeted liposomes. Preparation, characterization and hydroxyapatite binding in vitro. *Int J Pharm.* 2007;331:224–227.
25. Salerno M, Cenni E, Fotia C, et al. Bone-targeted doxorubicin-loaded nanoparticles as a tool for the treatment of skeletal metastases. *Curr Cancer Drug Targets*. 2010;10:649–659.
26. Swami A, Reagan MR, Basto P, et al. Engineered nanomedicine for myeloma and bone microenvironment targeting. *Proc Natl Acad Sci U S A*. 2014;111:10287–10292.
27. Mussi SV, Silva RC, Oliveira MC, Lucci CM, Azevedo RB, Ferreira LA. New approach to improve encapsulation and antitumor activity of doxorubicin loaded in solid lipid nanoparticles. *Eur J Pharm Sci*. 2013;48:282–290.
28. Pinkerton NM, Grandeury A, Fisch A, Brozio J, Riebesehl BU, Prud'homme RK. Formation of stable nanocarriers by in situ ion pairing during block-copolymer-direct rapid precipitation. *Mol Pharm*. 2013;10:319–28.
29. Stahl PH, Wermuth CG. *Handbook of Pharmaceutical Salts: Properties, Selection and Use*. 1st ed. Weinheim: Whiley-VCH; 2002.
30. Diniz SOF, Siqueira CF, Nelson DL, Martin-Comin J, Cardoso VN. ^{99m}Technetium-ceftizoxime kit preparation. *Brazilian Archives of Biology and Technology*. 2005;48:89–96.
31. Hung GU, Tsai SC, Kao CH, Lin WY, Wang SJ. Disparate results between I-131 and Tc-99m pertechnetate owing to administration of iodine-containing radiographic contrast material. *Semin Nucl Med*. 2000;30:147–148.
32. Ziessman HA, O'Malley JP, Thrall JH, Fahey FH. *Nuclear Medicine: The requisites. 4th ed*. Philadelphia: Elsevier; 2014.
33. Awasthi V, Goins B, Klipper R, Loredo R, Korvick D, Phillips WT. Imaging experimental osteomyelitis using radiolabeled liposomes. *J Nucl Med*. 1998;39:1089–1094.
34. Crommelin DJ, van Rensen AJ, Wauben MH, Storm G. Liposomes in autoimmune diseases: selected applications in immunotherapy and inflammation detection. *J Control Release*. 1999;62:245–251.
35. Erdogan S, Ozer AY, Ercan MT, Hincal AA. Scintigraphic imaging of infections with 99m-Tc-labelled glutathione liposomes. *J Microencapsul*. 2000;17:459–465.
36. Litzinger DC, Buiting AM, van Rooijen N, Huang L. Effect of liposome size on the circulation time and intraorgan distribution of amphipathic poly(ethylene glycol)-containing liposome. *Biochim Biophys Acta*. 1994;1190:99–107.
37. New RRC. *Liposomes: a practical approach*. 1st ed. Oxford: Oxford University Press; 1990.
38. Kurniawan J, Yin NN, Liu GY, Kuhl TL. Interaction forces between ternary lipid bilayers containing cholesterol. *Langmuir*. 2014;30:4997–5004.
39. Rannger C, Helbok A, von Guggenberg E, et al. Influence of PEGylation and RGD loading on the targeting properties of radiolabeled liposomal nanoparticles. *Int J Nanomedicine*. 2012;7:5889–5900.
40. Rauscher A, Frindel M, Maurel C, et al. Influence of pegylation and hapten location at the surface of radiolabelled liposomes on tumour immunotargeting using bispecific antibody. *Nucl Med Biol*. 2014;41 Suppl:e66–e74.
41. Phillips WT. Delivery of gamma-imaging agents by liposomes. *Adv Drug Deliv Rev*. 1999;37:13–32.
42. Ulrich AS. Biophysical aspects of using liposomes as delivery vehicles. *Biosci Rep.* 2002;22:129–150.
43. Gomes Barreto V, Iglesias F, Roca M, Tubau F, Martín-Comín J. [Labelling of ceftizoxime with 99m-Tc]. *Rev Esp Med Nucl*. 2000;19:478–483. Spanish.